Appl Microbiol Biotechnol (2014) 98:6431–6441
DOI 10.1007/s00253-014-5681-z

APPLIED MICROBIAL AND CELL PHYSIOLOGY

Sorption characteristics and mechanisms of Pb(II) from aqueous solution by using bioflocculant MBFR10543

Junyuan Guo · Jing Yu

Received: 9 February 2014 / Accepted: 4 March 2014 / Published online: 10 May 2014

Abstract This paper focuses on the effectiveness of removing Pb(II) from aqueous solution using bioflocculant MBFR10543 and a series of experimental parameters including MBFR10543 dose, calcium ions concentration, solution pH, and temperature on Pb(II) uptake was evaluated. Meanwhile, the flocculation mechanism of MBFR10543 was discussed. Results have demonstrated that the removal efficiency of Pb(II) reached 94.7 % (with the sorption capacity of 81.2 $mg \cdot g^{-1}$) by adding MBFR10543 in two stages, separately, 3×10^{-2} % (w/w) in the 1.0 min's rapid mixing (180 rpm) and 4×10^{-2} % (w/w) after 2.0 min's slow mixing (80 rpm) with pH value fixed at 6. Pb(II) flocculation process could be described by the Langmuir isotherms model and pseudo-second-order kinetic model. The negative Gibbs free energy change indicated the spontaneous nature of the flocculation. Fourier transform infrared spectra analysis indicated that functional groups, such as –OH, C=O, and C–N, were existed in MBFR10543 molecular chains, which had strong capacity for removing Pb(II). Furthermore, both charge neutralization and bridging being the main mechanisms involved in Pb(II) removal by MBFR10543.

Keywords Bioflocculant MBFR10543 · Pb(II) · Sorption · Flocculation mechanism

Introduction

It is well recognized that heavy metals discharged into surface water, such as Pb(II), Cr(VI), Cu(II), Zn(II), Cd(II), etc., are hazardous to human and the other living organisms owing to their accumulation in living tissues throughout the food chain as nonbiodegradable pollutants, even if small quantities (Sari et al. 2007). Thus, the removal of heavy metals from waters and wastewaters is extremely important. Pb(II), exists in the wastewater of many industries, like electric battery manufacturing, plating, tanneries, oil refining, smelting, and mining, is a potent neurotoxic and carcinogenic metal, whose pollution is of major concern (Boudrahem et al. 2011; Lodeiro et al. 2006). The presence of Pb(II) in drinking water, even at low concentrations, may cause human diseases like anemia, hepatitis, kidney failure, nervous diseases, etc. (Dumitru and Laura 2013; Feng et al. 2013; Wan et al. 2010). Therefore, the removal of excess Pb(II) from wastewater is of great significance for protecting human health as well as the environment.

A number of techniques have been applied to remove Pb(II) from wastewater for decades, such as precipitation, filtration, electroplating, and coagulation (Fu and Wang 2011; Jiang et al. 2010; Karatas 2012). However, these processes pose a significant problem in terms of the disposal of precipitated toxic sludge/waste products (Chakravarty et al. 2010; Meunier et al. 2006; Witek-Krowiak et al. 2011). Further, ion-exchange treatments are also available, which do not appear to be economical (Pehlivan and Altun 2006). It has been reported that wood materials, agricultural by-products, clay, natural zeolite, and other low-cost adsorbents have the capacity to adsorb and accumulate heavy metals, and the sorption capacities are found to be ranging from 3.04 to 425 $mg \cdot g^{-1}$ for Pb(II) (Karatas 2012). However, the uses of these materials have the disadvantage of increasing the chemical oxygen demand (COD) of water (Bai and Abraham 2003). As a result of this problem with the aforementioned solutions, it becomes necessary to find an effective and environment friendly process to remove Pb(II) from industrial wastewater.

J. Guo (✉) · J. Yu
College of Resources and Environment, Chengdu University of Information Technology, Chengdu, Sichuan 610225, China
e-mail: gjy@cuit.edu.cn

J. Guo
e-mail: guojunyuan08@163.com

Biosorption, which utilizes the ability of biological materials to bind and sequester heavy metals from aqueous solutions, is a considerable alternative process because of its good performance (Velmurugan et al. 2010). Many biological materials such as fungus *Aspergillus niger* and seaweeds have shown potential for the removal of heavy metal (Senthilkumar et al. 2007). Microbial bioflocculants (MBFs), secreted by microorganisms during their active secretion and cell lysis, is a kind of environment friendly material with the character of harmless and biodegradable, which has been considered as a potential solution to the toxicity to aquatic life and environment pollution in recent years (Li et al. 2009; Liu et al. 2010; Sun et al. 2012). Broadly, due to the special properties (sorption capability and degradability), MBFs have attracted wide attention in wastewater treatment, drinking water purification and downstream processes in biotechnology (You et al. 2008). MBFs belong to a kind of extracellular polymeric substances that are complex mixtures of macromolecular polyelectrolytes, depending on the chemical composition and structure, they exhibit ability to bind with metal ions. Therefore, it is interesting to investigate the possible application of MBFs to remove heavy metals. For example, removal of Pb(II) and Cu(II) ions from aqueous solutions by bacterial strain from soil (Tunali et al. 2006), biosorption of Cu(II) and Cd(II) ions from aqueous solutions using *Botrytis cinerea* fungal byproducts (Akar et al. 2005), and so on.

Bioflocculant MBFR10543 is a kind of microbial flocculant harvested from alkaline-thermal (ALT) pretreated sludge. It is relatively effective, eco-friendly, simple, and inexpensive to operate in our previous studies (Guo et al. 2013, 2014). The main objective of this research was to investigate the effectiveness of MBFR10543 to remove Pb(II) from aqueous solution and explore the flocculation mechanism based on the experimental results. The Pb(II) removal potential of MBFR10543 was evaluated as a function of MBFR10543 dose, solution pH, and temperature. Following the Pb(II) flocculation experiment, the interactions between MBFR10543 and Pb(II) were investigated by Fourier transform infrared spectra (FT-IR) and environmental scanning electron microscope (ESEM) analysis to determine the flocculation characteristics. Bonding mechanism was detected by adding 20 ml EDTA (3.0 $mol \cdot l^{-1}$) or CH_4N_2O (3.0 $mol \cdot l^{-1}$) into the stable Pb(II)-loaded MBFR10543 systems. Further, the Zeta potential during the flocculation process was also monitored to propose the flocculation mechanism.

Materials and methods

Reagents

$Pb(NO_3)_2$ (Hengxing Chemicals, China) was prepared by dilution of 1.0 $g \cdot l^{-1}$ stock solution, and the fresh diluents were used in each experiment. $CaCl_2$ (Hengxing Chemicals) was prepared at the concentration of 5.0 $g \cdot l^{-1}$. NaOH and HCl (Sanpu Chemicals, China) were prepared at the concentration of 1.0 $mol \cdot l^{-1}$. EDTA and CH_4N_2O (Fuchen Chemicals, China) were prepared at the concentration of 3.0 $mol \cdot l^{-1}$. Unless otherwise stated, all reagents used were analytically pure.

Bacteria strain and bioflocculant MBFR10543

Bioflocculant-production strain, *Rhodococcus erythropolis*, was deposited in China Center for Type Culture Collection (CCTCC) (No. ACCC.10543). Bioflocculant MBFR10543, a kind of microbial flocculant, was harvested from alkaline-thermal (ALT) pretreated sludge with suspended sludge solids concentration of 25 $g \cdot l^{-1}$ by *R. erythropolis*; this sludge was collected from biofiltration unit at a swine wastewater treatment plant located in Fuhua pig farm, Hunan Province, China (Guo et al. 2014).

Sludge treatments disintegrated the organic fractions and released soluble carbon into the sludge medium. Carbon sources and nitrogenous organic materials available in sludge medium changed with different treatment methods and therefore could change bioflocculants secretion pattern and yields. Thus, before bioflocculant production, the sludge suspensions were treated by sterilization (ST), alkaline-thermal (ALT) and acid-thermal (ACT) treatments, respectively. Sterilization was carried out by autoclaving (steam sterilization) at 121 °C for 30 min. In ALT treatment, first, pH value of the sludge solution was raised to 10 by using 1.0 $mol \cdot l^{-1}$ NaOH at room temperature (25 °C) and then autoclaved in the same procedure. In ACT treatment, first, pH value was reduced to 2.0 using 1.0 $mol \cdot l^{-1}$ HCl at room temperature (25 °C) and then autoclaved in the same procedure. After autoclaving, pH value of all the sludge samples were adjusted to 7.0 using 1.0 $mol \cdot l^{-1}$ HCl or NaOH. In our previous study, the specific carbon and nutrients content released in the ALT sludge medium was more favorable to bioflocculants secretion as compared to that of ST and ACT sludge (Guo et al. 2013, 2014).

Flocculation and sorption tests

A standard Jar Tester was used for the flocculation tests in $Pb(NO_3)_2$ solution dosed with MBFR10543. $CaCl_2$ and MBFR10543 were added into 1.0 l of $Pb(NO_3)_2$ solution in 1.0 l beaker in turn and then fixed on the floc-tester (ET-720, Lovibond, Germany). The pH of the mixture was adjusted using 1.0 $mol \cdot l^{-1}$ NaOH or HCl. MBFR10543 was added in two stages into the Pb(II) solution, separately, before rapid mixing (first stage) and after 2-min slow mixing (second stage). Flocculation was the first stage, began with 1.0 min rapid mixing at 180 rpm and ended with 2.0-min slow mixing at 80 rpm. The slow mixing after the first stage was the second

stage, about sorption. After the two stages' stirring, the mixture was allowed to stand to establish its equilibrium. The influence of the flocculation parameters including solution pH and doses of MBFR10543 and $CaCl_2$ was investigated by analyzing the removal efficiency of Pb(II) and the Zeta potentials of the flocculation systems. The concentrations of Pb(II) were determined by flame atomic adsorption spectrometry (Modle Analyst 700, Perkin-Elmer, USA) after being filtered by 0.45 μm filter membrane (APHA 2005). The experiments were performed at room temperature (25 °C). The removal efficiency (RE) and removal capacity of Pb(II) was calculated as follows:

$$\mathrm{RE}(\%) = (\mathrm{C}_0 - \mathrm{C}_e)/\mathrm{C}_0 \times 100 \quad (1)$$

$$\text{Removal capacity} = (\mathrm{C}_0 - \mathrm{C}_e)\mathrm{V}/\mathrm{W}_\mathrm{R} \quad (2)$$

where C_0 and C_e are the initial and equilibrium Pb(II) concentrations (milligram per liter), respectively, V is the volume of the $Pb(NO_3)_2$ solution (liter), and W_R is the weight of MBFR10543 used (gram).

Following Pb(II) sorption experiments, isotherms, kinetics, and thermodynamics were described, and the bonding mechanism was detected by adding 20 ml EDTA (3.0 $mol \cdot l^{-1}$) or CH_4N_2O (3.0 $mol \cdot l^{-1}$) into the stable Pb(II)-loaded MBFR10543 systems. The variation of Zeta potential during the process of flocculation was monitored by Zetasizer 2000 (Malvern Instruments, England). Samples were carried out at different time points: $Pb(NO_3)_2$ solution at pH 6, after adding MBFR10543, after adding $CaCl_2$ and during flocculation process. All experiments were performed in triplicates for the mean calculation.

Isotherms, kinetics, and thermodynamics studies

Isotherm fitting with model equations is a key issue to explore flocculation mechanisms, and the Langmuir and Freundlich models were applied to understand the sorption behavior of Pb(II) during Pb(II) flocculation process (Sari and Tuzen 2008; Sari et al. 2008). The Langmuir isotherm assumes that adsorption occurs at specific homogeneous sites within the adsorbent and can be saturated as Eq. (3).

$$\frac{C_\mathrm{e}}{q_\mathrm{e}} = \frac{1}{k_\mathrm{L} q_\mathrm{m}} + \frac{C_e}{q_m} \quad (3)$$

where q_e and q_m (milligram per gram) are the equilibrium and maximum sorption capacity of Pb(II), and k_L (liter per milligram) is the Langmuir constant which is related to the affinity of the binding sites.

The essential feature of the Langmuir isotherm can be expressed by means of a separation factor or equilibrium parameter R_L, which is calculated by the Eq. (4). There are four probabilities for the R_L value: (i) for favorable exchange, $0<R_L<1$; (ii) for unfavorable exchange, $R_L>1$; (iii) for linear exchange, $R_L=1$; and (iv) for irreversible exchange, $R_L=0$ (Riahi et al. 2009).

$$R_\mathrm{L} = \frac{1}{1 + k_\mathrm{L} C_\mathrm{e}} \quad (4)$$

The Freundlich isotherm is based on multilayer sorption by assuming that the adsorbent has a heterogeneous surface with non-uniform distribution of sorption sites (Widiastuti et al. 2011), and the liner form of the Freundlich isotherm equation is normally given as Eq. (5):

$$\log q_\mathrm{e} = \log k_\mathrm{f} + \frac{1}{n} \log C_\mathrm{e} \quad (5)$$

where k_f and $1/n$ represent the Freundlich capacity coefficient and the Freundlich intensity parameter, respectively, and $1/n$ is also known as the heterogeneity factor.

Isotherm studies were conducted by contacting $3\times10^{-2}+4\times10^{-2}$ % (w/w) MBFR10543 into 1.0 l Pb(II) solution at concentration of 60 $mg \cdot l^{-1}$ with the solution stirring in two stages. The experiments were performed at different temperatures (25, 35, and 45 °C) by water bath. Sorption isotherms are plots of the equilibrium sorption capacity (q_e) (according to Eq. (2)) versus the equilibrium concentration of the residual Pb(II) in the solution (C_e). The equilibrium uptake was calculated by Eqs. (6) and (7).

$$q_\mathrm{e} = (\mathrm{C}_0 - \mathrm{C}_\mathrm{e})\mathrm{V}/\mathrm{W} \quad (6)$$

$$\mathrm{W} = (\mathrm{C}_0 - \mathrm{C}_\mathrm{f})\mathrm{V} + \mathrm{W}_\mathrm{R} \quad (7)$$

where C_f (milligram per liter) is the concentration of Pb(II) after first stage. W (gram) is the weight of adsorbent. All the batch experiments were carried out in triplicate and the average values were presented (with standard error less than 5 % of the mean).

Kinetic models were always used to investigate the characteristics of sorption and its potential rate-controlling steps that include mass transport and chemical reaction processes (Anayurt et al. 2009; Sari and Tuzen 2009; Uluozlu et al. 2008). In addition to clarifying the sorption kinetics of Pb(II)

onto MBFR10543, two kinetic models, pseudo-first-order and pseudo-second-order were applied, and the equations were determined by Eqs. (8) and (9). Kinetic studies were conducted by contacting $3\times10^{-2}+4\times10^{-2}$ % (w/w) MBFR10543 into 1.0 l Pb(II) solution at different initial concentrations (40, 50, and 60 mg·l^{-1}) with the samples stirring for designated time. The experiments were performed at temperature of 25 °C.

$$\log(q_t - q_e) = \log q_e - \frac{k_1}{2.303}t \tag{8}$$

$$\frac{t}{q_t} = \frac{1}{k_2 {q_e}^2} + \frac{t}{q_e} \tag{9}$$

where q_t (mg·g^{-1}) is the amount of adsorbed Pb(II) at time t, and k_1 (min^{-1}) and k_2 (g·mg^{-1}·min^{-1}) are the rate constants of the pseudo-first-order and pseudo-second-order models, respectively.

Effects of sorption temperature on the flocculation of Pb(II) were given from the calculated thermodynamic parameters (Liu and Liu 2008; Lu 2008), and the thermodynamic data such as enthalpy (ΔH^o), free energy change (ΔG^o) and entropy (ΔS^o) can be calculated by Eqs. (10)–(13).

$$\Delta G^o = -RT\ln K \tag{10}$$

$$\frac{d\ln K}{d\left({}^1/_T\right)} = -\frac{\Delta H^o}{RT^2} \tag{11}$$

$$d\left(\frac{\Delta G^o}{T}\right) = -\frac{\Delta H^o}{T^2}dT \tag{12}$$

$$\Delta G^o = \Delta H^o - T\Delta S^o \tag{13}$$

where K is the equilibrium constant (liter per gram), R is the universal gas constant (8.314 J·mol^{-1}·K^{-1}), and T is the temperature (Kelvin).

FT-IR spectra and ESEM analysis

To investigate the characteristics of the flocculation process including the mechanism involved, the FT-IR and ESEM profiles were studied. Fourier transform-infrared spectrometer (EQUINOX 55, Bruker, Germany) was employed to examine the interactions between the Pb(II) and functional groups on MBFR10543. Original samples and flocs which MBFR10543 flocculated Pb(II) under the optimal experimental conditions were collected, followed by vacuum freeze-drying. The samples were ground well to make KBr pellets under hydraulic pressure of 400 kg·cm^2, and spectra were recorded in the range of 400–4,000 cm^{-1}. In each scan, the amounts of the sample and KBr were kept constant in order to know the changes in the intensities of characteristic peaks with respect to the structural changes. ESEM (Quanta 200 FEG, FEI, USA) was applied to analyze the surface morphology of original and Pb(II)-loaded MBFR10543 in low vacuum mode at an acceleration potential of 20 keV. Furthermore, microanalysis of the Pb(II)-loaded MBFR10543 was carried out with an energy-dispersive spectrometer (EDS) equipped on the Quanta 200.

Results

Removal efficiency and removal capacity in different experiment conditions

Effects of MBFR10543 dose on the flocculation behavior

The effects of MBFR10543 dose on the flocculation of Pb(II) was investigated by adding different mass fractions of MBFR10543 into 1.0 l $Pb(NO_3)_2$ solution (60 mg·l^{-1}) with pH value fixed at 6. MBFR10543 was added before rapid mixing (first stage) and after 2-min slow mixing (second stage). As can be seen from Fig. 1a, at the first stage, the removal efficiency of Pb(II) increased to 65.2 % when 3×10^{-2} % (w/w) MBFR10543 was added and then decreased with increasing addition of MBFR10543. Less dose of MBFR10543 meant less MBFR10543 molecules adsorbed Pb(II), and fewer bridges were developed between them. Further increase of MBFR10543 led to a drastic decrease of the removal efficiency of Pb(II), because more doses of MBFR10543 would inhibit small flocs to grow into big ones. As a result of stronger repulsion force between flocs, they could be deflocculated. After the first stage, the residential concentration of Pb(II) was still high (20.9 mg·l^{-1}), so MBFR10543 needed to be added continuously based on the preliminary tests. At the second stage, the removal efficiency of Pb(II) reached about 94.2 % when the addition of MBFR10543 was adjusted to 4×10^{-2} % (w/w). The removal capacity showed the same tendency to removal efficiency after the second stage, and a maximum value of 80.8 mg·g^{-1} was achieved. This dosing method of MBFR10543 in two stages was similar with that in the Pb(II) removal process by MBFGA1 (Feng et al. 2013). Like flocculating MBFGA1,

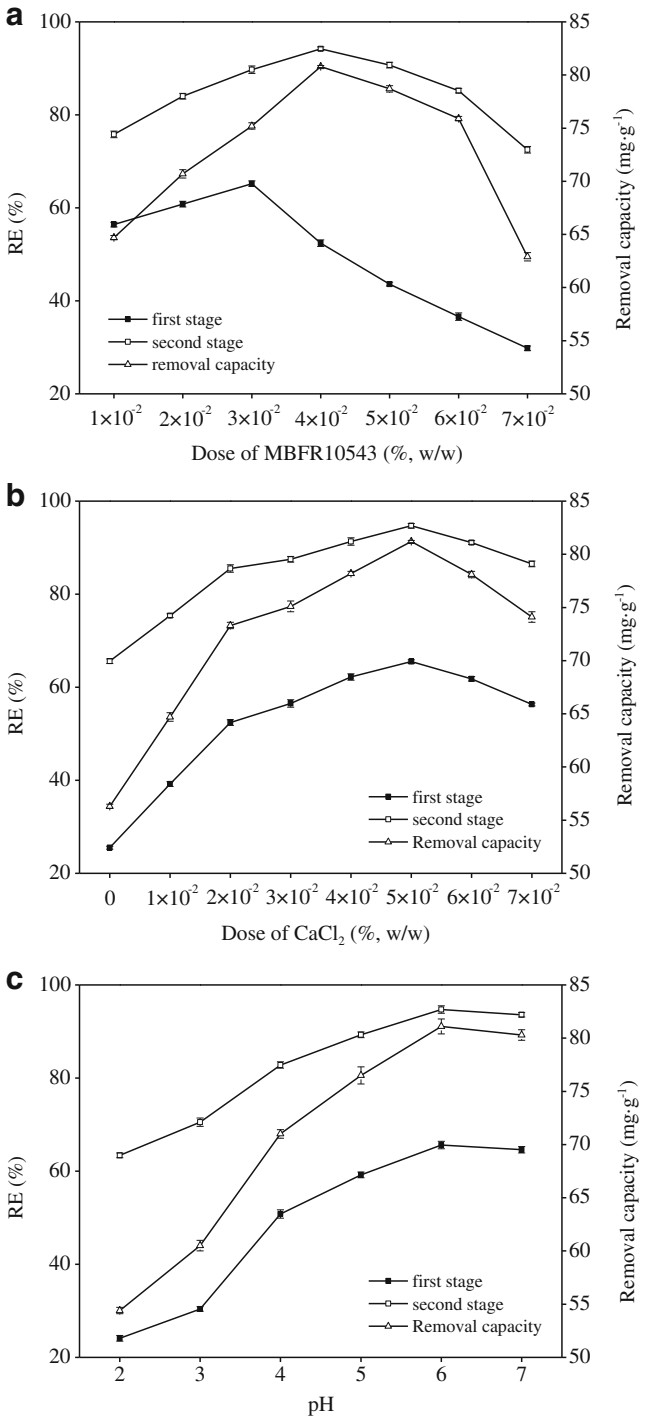

Fig. 1 Effect of **a** MBFR10543 dose, **b** $CaCl_2$ dose, and **c** solution pH on the removal of Pb(II)

the dose of MBFR10543 should be optimized because more or less dose would be unfavorable to the flocculation.

Effects of $CaCl_2$ dose on the flocculation behavior

The effect of $CaCl_2$ on the flocculating efficiency of Pb(II) was investigated by adding different volumes of $CaCl_2$ and $3\times10^{-2}+4\times10^{-2}$ % (w/w) MBFR10543 into 1.0 l $Pb(NO_3)_2$ solution (60 $mg\cdot l^{-1}$) with pH value fixed at 6. Fig. 1b indicated that the removal efficiency of Pb(II) was low without adding $CaCl_2$. With further addition of $CaCl_2$, the removal efficiency of Pb(II) increased, and the maximum value of 81.2 $mg\cdot g^{-1}$ was achieved after 5×10^{-3} % (w/w) $CaCl_2$ added. During the flocculating process, as a kind of coagulant aid, Ca^{2+} increases the initial sorption capacity of MBFR10543 by decreasing the negative charge on the polymer. It has also been reported to develop bridges between anionic polyelectrolytes and negatively charged colloidal particles, thereby enhancing particle flocculation (Lee et al. 2012). These two mechanisms have been detected in our previous studies (Guo et al. 2013, 2014), flocculating activity of kaolin clay suspension was enhanced to 94.5 % by adding 20 mg of bioflocculant in the presence of 0.5 g Ca^{2+}, while a flocculating activity of 44.7 % was achieved when 20 mg of the bioflocculant was added into kaolin suspension (1.0 l) alone and only 17.2 % reached when 0.5 g Ca^{2+} was added alone.

Effect of pH value on the flocculation behavior

Solution acidity was an important factor on the flocculation of Pb(II) for both solution chemistry of Pb(II) and surface characteristics of MBFR10543. It directly related with the competition between hydrogen ions (H^+) and Pb(II) to get adsorbed to active sites and also the activity of the functional groups present on the MBFR10543 surface that are responsible for Pb(II) removal (Pehlivan et al. 2009; Huang and Liu 2013). The functional groups not only disturbed the combining force for Pb(II) in solution but also were involved in the ion-exchange of Pb(II) on the MBFR10543. So the removal of Pb(II) was highly dependent on the pH value of aqueous solution. The pH optimization study was carried out by adding 5×10^{-3} % (w/w) $CaCl_2$ and $3\times10^{-2}+4\times10^{-2}$ % (w/w) MBFR10543 into 1.0 l $Pb(NO_3)_2$ solution (60 $mg\cdot l^{-1}$), and the results were presented in Fig. 1c. In order to avoid the precipitation in alkaline condition, the flocculation of Pb(II) was carried out in acid condition (pH 2–7) in this study. As shown in Fig. 1c, the Pb(II) removal is positively correlated with the increase of pH value in the solution, reaching a maximum removal efficiency of 94.7 % (with the sorption capacity of 81.2 $mg\cdot g^{-1}$) at pH 6. Similar values of optimum pH (6.2) for Pb(II) removal have been reported in the literature using pestan (an extracellular polysaccharide) (Moon et al. 2006). Additionally, the removal capacity of MBFR10543 for Pb(II) (81.2 $mg\cdot g^{-1}$) was higher than majority of other biosorbents that have been mentioned (12.3-72.5 $mg\cdot g^{-1}$) on relevant works previously (Table 1). Therefore, it could be noteworthy that MBFR10543 has important potential for the removal of Pb(II) from aqueous solution.

Table 1 Biosorbents used for Pb(II) removal capacity (milligram per gram)

Biosorbents	Removal capacity	References
Pestalotiopsis sp.	51.9	Moon et al. (2006)
Saccharomyces cerevisiae	30.1	Cabuk et al. (2007)
Lichen (*Cladonia furcata*)	12.3	Sari et al. (2007)
Barley straws	23.2	Pehlivan et al. (2009)
Penicillium sp.	72.5	Velmurugan et al. (2010)
Pseudomonas sp.	69.8	Huang and Liu (2013)
Solanum melongena leaf	55.6	Yuvaraja et al. (2014)
MBFR10543	81.2	This study

Isotherms, kinetics, and thermodynamics parameters

The isotherms data were obtained by linear regression method and were summarized in Table 2. Within the studied temperature range (25, 35, and 45 °C), the isotherms data exhibited higher correlation with Langmuir model than Freundlich model (based on the higher correlation coefficient, i.e., R^2 values). From Langmuir model, the q_m values decreased with the rising temperature, this suggested the affinity between the active sites of the MBFR10543 and Pb(II) and also between the adjacent molecules of the adsorbed phase would be stronger at higher temperature in comparison to lower temperature (Feng et al. 2013; Ghorai et al. 2012). Additionally, all the R_L values that were obtained between 0 and 1 indicated that the removal of Pb(II) by MBFR10543 was propitious; this implied that the Langmuir equation was able to properly describe the equilibrium isotherm of Pb(II) adsorbed onto MBFR10543. The fact that the data did not fit well with the Freundlich isotherm indicates that Pb(II) removal is more like a monolayer surface sorption process with finite number of identical sites, which were homogeneously distributed on MBFR10543 surface. From Freundlich model, the obtained values of 1 / *n* are lower than 1 which suggests that the removal of Pb(II) by the MBFR10543 is substantially favorable.

The model rate constants, correlation coefficients, and calculated q_e values of the two kinetics models for the sorption of Pb(II) onto MBFR10543 at various initial concentrations were tabulated in Table 3. It was found that correlation coefficients values of pseudo-first-order equation were relatively low within the studied Pb(II) concentrations' range, indicating the bad linearization, yet these values of pseudo-second-order equation were extremely high and all greater than 0.99. Besides, the calculated q_e values of pseudo-second-order equation matched very well with the experimental data. These results suggested that the sorption of Pb(II) onto MBFR10543 followed well the pseudo-second-order model. Thus, experiment results supported the assumption that the rate-limiting step in sorption of heavy metals are chemisorption involving valence forces through the sharing or exchange of electrons between adsorbent and metal ions. Additionally, it is worthwhile to note that k_1 and k_2 have higher values at a higher initial Pb(II) concentration, which leads to a higher driving force for the sorption of Pb(II), hence a higher sorption capacity.

The effects of temperature on the sorption of Pb(II) onto MBFR10543 was given from the calculated thermodynamic parameters (Table 4). It is clear that the values of ΔG^o were negative at various temperatures (−5.46, −6.82, and −8.09 kJ·mol^{-1} at 25, 35, and 45 °C, respectively) with Pb(II) concentration of 60 mg·l^{-1}, confirming that the sorption of Pb(II) onto MBFR10543 was spontaneous in nature and thermodynamically favorable, and no energy input to the system is required. It is worth noting that ΔG^o values became more negative as temperature increased, the increase in ΔG^o values with increased temperature showed an increase in driving force for Pb(II) sorption at higher temperature. The positive values of ΔH^o indicated that the sorption was enothermic process at 25–45 °C. The positive values of ΔS^o confirmed the increased randomness at solid/solution interface during the flocculation process.

Flocculation mechanism

FT-IR analysis

The studies so far indicated that MBFR10543 can be successfully used for the removal of Pb(II) from aqueous solution. An effort was made to identify the components of the MBFR10543 that are responsible for Pb(II) removal. Hence, the nature of the possible Pb(II)-MBFR10543 interactions was elucidated on the basis of FT-IR, and the FT-IR spectra of

Table 2 Parameters for Langmuir and Freundlich isotherms for Pb(II) removal by MBFR10543

Temperature (Kelvin)	Langmuir isotherms				Freundlich isotherms		
	q_m (milligram per gram)	k_L (liter per milligram)	R_L	R^2	k_f (milligram per gram)	1 / *n*	R^2
298	24.27	1.01	0.016	0.9666	16.41	0.190	0.8987
308	22.17	0.49	0.033	0.9159	12.88	0.226	0.8796
318	21.55	0.33	0.048	0.9009	4.39	0.577	0.8863

Table 3 Pseudo-first-order and pseudo-second-order parameters for Pb(II) removal by MBFR10543

C_0 (milligram per liter)	Pseudo-first-order			Pseudo-second-order		
	k_1 (per minute)	q_e (milligram per gram)	R^2	k_2 (gram per milligram per minute)	q_e (milligram per gram)	R^2
50	0.089	20.61	0.9239	0.022	72.99	0.9991
60	0.090	21.48	0.9089	0.021	75.21	0.9992
70	0.091	22.18	0.9242	0.020	75.76	0.9996

original and Pb(II)-loaded MBFR10543 in the range of 4,000–400 cm^{-1} were taken and presented in Fig 2 and Table 5. The complex spectra in Fig 2 show several strong sorption bands, which were assigned on the basis of the structure of the MBFR10543 and were facilitated by the available data of FT-IR spectra. The FT-IR spectrum of Pb(II)-free form showed several distinct and sharp peaks at 3,378 cm^{-1} (indicative of –OH and $–NH_2$ functional groups), 2,930 cm^{-1} (indicative of C–H groups), 1,651 cm^{-1} (indicative of –C=O groups), 1,455 cm^{-1} (indicative of the bending of $–CH_3$), 1,265 cm^{-1} (indicative of C–N groups in amide band of the protein peptide bond), and 1,060 cm^{-1} (indicative of C–O groups) (Huang et al. 2012; Feng et al. 2013). In conclusion, the Fourier transform infrared spectra (FTIR) spectrum of the Pb(II)-free MBFR10543 showed the presence of hydroxyl, carboxyl, and amine groups, which always played important roles in Pb(II) removal. The significant shifts of the wave number and intensity of these specific peaks after Pb(II) sorption from the spectra of Pb(II)-loaded MBFR10543, suggesting the aforementioned functional groups were mainly involved in the sorption of Pb(II) onto MBFR10543 (Sari et al. 2007). After loading Pb(II), the peaks of hydroxyl (−OH) groups shifted from 3,378 to 3,364 cm^{-1}; this significant shifts of –OH peak to the lower wave number after the Pb(II) sorption suggested that chemical interactions between the Pb(II) and –OH groups occurred on the MBFR10543 surface and the hydrogen bonding of the hydroxyl groups decreases after Pb(II) loading. The shifts of C=O from 1,651 to 1,655 cm^{-1} in the Pb(II)-loaded MBFR10543 can be assigned to the carboxylate ion ($-COO^-$). The shifts of C–N implied the involvement of amide groups in the flocculation process of Pb(II). All the conspicuous change in the FTIR spectrum demonstrated that the chemical interactions, between Pb(II) and the amine, carboxyl, and hydroxyl groups of MBFR10543, were mainly involved in the flocculation process of Pb(II). The results were in good agreement with those obtained by other researchers (Chen et al. 2008; Yahya et al. 2012), which all came to the conclusion that functional groups responsible for Pb(II) removal were mainly carboxyl, hydroxyl, and amine groups.

Table 4 Thermodynamic parameters for Pb(II) removal by MBFR10543

C_0 (milligram per liter)	ΔG^o (kilojoule per mole)			ΔH^o (kilojoule per mole)	ΔS^o (kilojoule per mole)
	298 K	308 K	318 K		
50	−3.51	−5.05	−7.79	24.49	0.101
55	−4.73	−5.96	−7.91	25.06	0.103
60	−5.46	−6.82	−8.09	25.42	0.105
65	−5.17	−6.09	−7.68	23.55	0.099
70	−4.24	−5.25	−7.03	22.12	0.092

ESEM analysis

To investigate the flocculation process further, the original and Pb(II)-loaded MBFR10543 were observed under the ESEM. In secondary electron mode, ESEM micrographs showed that the surface and the texture of Pb(II)-loaded MBFR10543 became rougher and more compact compared with the Pb(II)-free MBFR10543 prepared by vacuum freeze-drying, which characterized a stronger sorption capacity (Fig. 3). Content of 57.1 % in the detection area of Pb(II)-loaded MBFR10543 and the appearance of Pb(II) signal at about 2.3, 10.6, and 12.6 keV presented in Table 6 clearly demonstrated the presence of Pb(II) due to the sorption onto MBFR10543 and a strong coordination linkage between Pb(II) and functional groups involved in MBFR10543. For example, the intensity of the phosphorus signal at about 2.1 keV was considerably reduced after the Pb(II) sorption, this could be indicative of the complexation of Pb(II) with

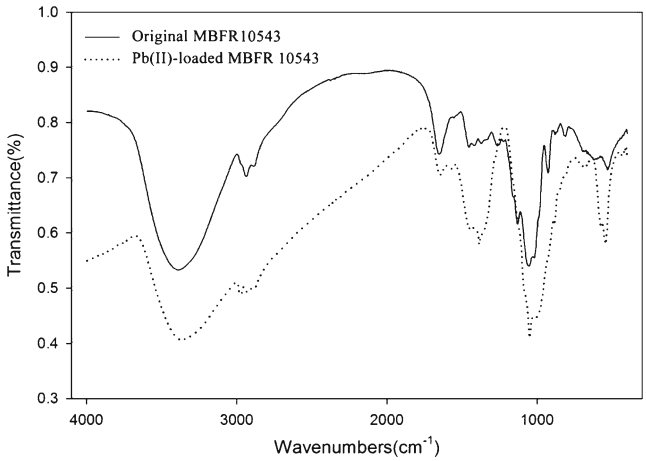

Fig. 2 FTIR spectrum of original and Pb(II)-loaded MBFR10543

Table 5 Wave number of FT-IR sorption peaks of original and Pb(II)-loaded MBFR10543

Functional groups	Original MBFR10543	Pb(II)-loaded MBFR10543
–OH and $–NH_2$	3,378	3,364
–C=O	1,651	1,655
–CH3	1,455	1,380
C–N	1,265	–
C–H	2,930	2,964
C–O	1,060	1,051

phosphate groups on the MBFR10543 surface. In addition, the disappearance of K signal at about 3.3 keV was observed after Pb(II) sorption indicated that flocculation and sorption process also included ion-exchange mechanism for Pb(II) removal (Cabuk et al. 2007).

Bonding and flocculation mechanism

MBFR10543 participates in the flocculation, mainly through hydroxyl, carboxyl, and amine groups, which induces very high binding capacity. In general, addition of EDTA and CH_4N_2O in the stable Pb(II)-MBFR10543-Ca^{2+} systems could destroy the ionic bonds or hydrogen bonds in the system, respectively. In this study, after addition of EDTA (3.0 mol·l^{-1}) into the stable system, the flocs dissolved gradually and became cloudy, while nothing happened by adding CH_4N_2O (3.0 mol·l^{-1}). The results indicated that ionic bond combination was the main way of combining between MBFR10543 and Pb(II), whereas the hydrogen-bonding interaction was not obvious.

Zeta potential and flocculation mechanism

The removal efficiency and Zeta potential of Pb(II) during flocculation process were shown in Fig. 4. At the first stage, the removal efficiency of Pb(II) increased rapidly, and then it increased steadily and reached equilibrium (94.7 %) after the second stage. The pH played an important role in the process. MBFR10543 had a linear long-chain molecular structure and appeared to have a molecular weight of 3.99×10^5 Da (Guo et al. 2013, 2014). With the increasing pH value of below 7, the MBFR10543 molecules stretch form a linear structure so that more of the active binding sites emerged, and the removal capacity of Pb(II) was bigger. It was found that the Zeta potential of $Pb(NO_3)_2$ solution was about 41.6 mV at pH 6 without Ca^{2+} and MBFR10543 additions, which turned to be 17.2 mV after adding 3×10^{-2} % MBFR10543 alone (without Ca^{2+}), and then 10.1 mV when 4×10^{-3} % $CaCl_2$ was added. As shown in Fig. 4, after the first stage, the Zeta potential appeared to be 8.7 mV. The addition of MBFR10543, which aroused a big reduction of about 25.9 mV in the Zeta potential of $Pb(NO_3)_2$ solution after the 1-min stirring, indicated that the charge neutralization would not be the main Pb(II) removal mechanism in this stage. Ca^{2+} reduced the thickness of the diffuse double layer of adjacent colloids, thus reducing the interparticle distance and making MBFR10543 attract more Pb(II) around its surface, and small flocs formed. The main Pb(II) removal mechanism involved in the second stage was sorption, in which bridging occurred after Pb(II) and Ca^{2+}

Table 6 EDS analysis of original and Pb(II)-loaded MBFR10543

Element	Original MBFR10543		Pb(II)-loaded MBFR10543	
	Energy (kiloelectron volt)	wt.%	Energy (kiloelectron volt)	wt.%
C	0.3	58.3	0.3	13.3
O	0.6	24.9	0.6	17.8
P	2.1	4.8	2.1	6.1
S	2.3	0.5	–	–
K	3.2, 3.6	8.8	–	–
Na	1.2	0.8	1.2	0.5
Ca	–		3.5	3.5
Pb	–		2.3, 10.6, 12.6	57.1

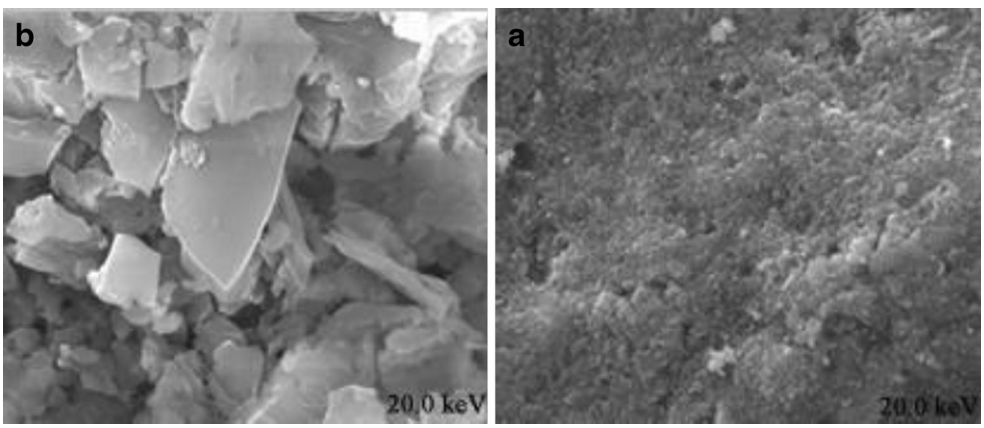

Fig. 3 ESEM micrographs of original MBFR10543 (**b**) and Pb(II)-loaded MBFR10543 (**a**)

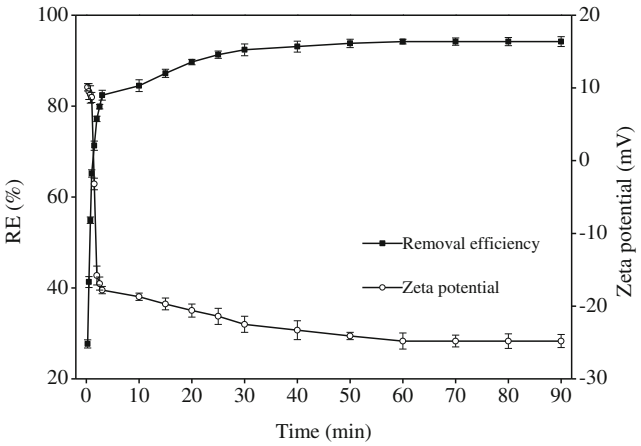

Fig. 4 Zeta potential and removal efficiency of Pb(II) during the sorption process

adsorbed onto MBFR10543. The fact that bridging played a major role during the second stage was confirmed by the occurrence of flocculation at a Zeta potential of about −24.8 mV. Many flocs could be adsorbed onto a long molecular chain, simultaneously, they could be absorbed by other polymer chains. Thus, flocs formed three-dimensional structure with a better settling capacity (Feng et al. 2013; More et al. 2012).

Discussion

The MBFR10543 appears as an effective and alternative microbial flocculant to be used for the removal of Pb(II) from wastewaters, and the maximum sorption capacity of 81.2 $mg \cdot g^{-1}$ can be reached when MBFR10543 was added in two stages, separately. For Pb(II) removal, the behavior of Pb(II) as a function of water's pH can be explained by considering the change in density of hydrogen ions (H^+) and the surface charge of MBFR10543. At pH values lower than 6, the removal efficiency of Pb(II) was in the range of 60–80 % and decreased with the decreasing solution pH value, which may be attributed to the increased density of H^+ corresponding to the decreasing pH value that could strongly compete with Pb(II) to get adsorbed on the binding sites which are responsible for Pb(II) (Nasir et al. 2007). Furthermore, the sorption was related to physicochemical interaction of the species in solution. Pb(II) removal was inhibited because the functional groups would be protonated at high acidic pH (low solution pH), thereby the strong resistance against Pb(II) binding. In contrast, when pH increases, more functional groups would be exposed (the active sites in MBFR10543) and efficiently release their protons into the solution to carry negative charges to enhance the Pb(II) sorption capacity. The effects of pH can also be explained in terms of pHpzc of the MBFR10543 (Yuvaraja et al. 2014). The pHpzc is an important characteristic for adsorbents to determine the pH at which the surface has net electrical neutrality. Surface charge of MBFR10543 is positive which results in low Pb(II) removal at water pH lower than pHpzc, and it is negative at water pH greater than pHpzc for attachment of Pb(II) to the surface to a greater extent. The pHpzc value of the MBFR10543 is found to be 2.5. Meanwhile, the surface charge of MBFR10543 determined by measuring its Zeta potential at different pH values showed that Zeta potential decreased from +3.93 to −27.80 mV, which was corresponding to the increase in pH from 2 to 7. This clearly indicated that at low pH values, the surface being positively charged would not be favorable for the attachment of positively charged Pb(II) due to electrostatic repulsion. With the increase of pH values, the cell surface became more negatively charged, favorable for Pb(II) removal. That is, at low pH values, increased positive charge (protons) density on the sites of MBF surface restricted the approach of Pb(II) as a result of repulsive force. In contrast, as the pH values increased, MBF surfaces were more negatively charged, and subsequently, sorption of the Pb(II) with positive charge was reached maximum around pH 5–7 (Karthikeyan et al. 2007).

To further investigate the reason for pH dependence of removal of Pb(II) by MBFR10543, FT-IR studies on the basis of the surface charge density at different pH values were performed for the original [Pb(II)-free form] and Pb(II)-loaded MBFR10543. Results have demonstrated that carboxyl, hydroxyl, and amine groups were mainly responsible for Pb(II) removal. The negative charge between pH 3 and 4 could develop due to the carboxyl group, whereas hydroxyl group was responsible for negative charges at pH values of 4–7. The positive charge at low pH (<3) might be attributed to the amine group on the MBFR10543 (Huang and Liu 2013). As the acidity decreased in the solution, the deprotonation of acid functional groups are strengthened, and in consequence, the numbers of attractions will increase between negative charge on MBFR10543 and Pb(II). Dissociation of the hydroxyl and carboxylic acid groups was at pK_a of 8–12 for hydroxyl and 3.8–5 for carboxylic groups (Pehlivan et al. 2009). Protonation of NH_2 to form NH_3^+ was at lower pH. At pH greater than 4, the carboxylic acid group is converted to the $-COO^-$, and Pb(II) is adsorbed. The involvement of carboxylic acid groups in the flocculation process explains the effect of pH on Pb(II) removal (see "Effect of pH value on the flocculation behavior" section). With the decreasing pH of below 4, majority of the carboxylate ions are converted to carboxylic acid groups (−COOH), and hence, the removal efficiency decreases (Gupta and Rastogi 2008). As more NH_2 groups were protonated to NH_3^+ form, there were only fewer NH_2-binding sites on the surface of MBFR10543–NH_2 for Pb(II) sorption (Hao et al. 2010). The functional groups, such as –

OH, −COOH, and –NH_2 groups interaction with Pb(II), are shown as follows:

$$\mathrm{MBFR10543-OH \rightarrow MBFR10543-O^- + H^+} \quad (14)$$

$$\mathrm{MBFR10543-O^- + Pb^{2+} \rightarrow MBFR10543-O-Pb + H^+} \quad (15)$$

$$\mathrm{MBFR10543-COOH \rightarrow MBFR10543-COO^- + H^+} \quad (16)$$

$$\mathrm{MBFR10543-COO^- + Pb^{2+} \rightarrow MBFR10543-COO-Pb + H^+} \quad (17)$$

$$\mathrm{MBFR10543-NH_3{}^+ \rightarrow MBFR10543-NH_2 + H^+} \quad (18)$$

$$\mathrm{MBFR10543-NH_2 + Pb^{2+} \rightarrow MBFR10543-NH_2\,Pb^{2+}} \quad (19)$$

$$\mathrm{MBFR10543-NH_3{}^+ + Pb^{2+} \rightarrow MBFR10543-NH_2\,Pb^{2+} + H^+} \quad (20)$$

EDTA (3.0 $\mathrm{mol \cdot l^{-1}}$) should be able to compress the electrical double layer of the colloidal particles, and bridging occurred between EDTA and MBFR10543, and thereby, the cloudy Pb(II)-MBFR10543-Ca^{2+} systems could be restabilized. However, the experimental results showed that the cloudy systems did not settle in 30 min, indicating Ca^{2+} played a binding role of the bridging in the flocculation process. After addition of the EDTA, the ionic bonds in the bridging were destroyed and the stable system became cloudy due to the strong coordination between EDTA and Ca^{2+} (complex stability constant log β_1 as high as 11.0). If there were hydrogen bonds in the bridging, they could be destroyed in the CH_4N_2O solution, and new hydrogen bonds formed, and thereby, the stable system became cloudy. After addition of 3.0 $\mathrm{mol \cdot l^{-1}}$ CH_4N_2O, there was no significant deflocculation phenomenon, indicating that the hydrogen-bonding interactions was not obvious.

The flocculation of Pb(II) was completed by charge neutralization and bridging mechanism in two stages: coagulation and sorption. The first stage was the coagulation, in which MBFR10543 attract Pb(II) around its surface by reducing the thickness of the diffuse double layer of adjacent colloids and thus reducing interparticle distance by addition of Ca^{2+}. The second stage was sorption, in which slow mixing allowed the aggregates to combine two or more flocs to form larger floc particles and precipitate as evidenced in the jar tests. Futher, the FT-IR, ESEM, and desorption analysis (bonding testing experiments) illustrated that chemical reaction also happened during flocculation process.

All in all, the MBFR10543 appears as an effective and alternative microbial flocculant to be uesd for the removal of Pb(II) from wastewaters by adding in two stages, separately. Pb(II) was adsorbed through bridging mechanism, and carboxyl, hydroxyl and amine functional groups were involved in the process. Based on the results, MBFR10543 could be used as an efficient source of biomaterial to solve the serious problems caused by heavy metal ions pollution.

Acknowledgments Project (KYTZ201405) Supported by the Scientific Research Foundation of Chengdu University of Information Technology (CUIT).

References

Akar T, Tunali S, Kiran I (2005) *Botrytis cinerea* as a new fungal biosorbent for removal of Pb(II) from aqueous solution. Biochem Eng J 25:227–235

Anayurt RA, Sari A, Tuzen M (2009) Equilibrium, thermodynamic and kinetic studies on biosorption of Pb(II) and Cd(II) from aqueous solution by macrofungus (*Lactarius scrobiculatus*) biomass. Chem Eng J 151:255–261

APHA (2005) Standard methods for the examination of water and wastewater, 21st edn. APHA, Washington, DC

Bai RS, Abraham TE (2003) Studies on chromium(VI) adsorption–desorption using immobilized fungal biomass. Bioresour Technol 87: 17–26

Boudrahem F, Aissani-Benissad F, Soualah A (2011) Adsorption of lead (II) from aqueous solution by using leaves of date trees as an adsorbent. J Chem Eng Data 56:1804–1812

Cabuk A, Akar T, Tunali S, Gedikli S (2007) Biosorption of Pb(II) by industrial strain of *Saccharomyces cerevisiae* immobilized on the biomatrix of cone biomass of *Pinus nigra*: equilibrium and mechanism analysis. Chem Eng J 131:293–300

Chakravarty S, Mohanty A, Sudha TN, Upadhyay AK, Konar J, Sircar JK, Madhukar A, Gupta KK (2010) Removal of Pb(II) ions from aqueous solution by adsorption using bael leaves (*Aegle marmelos*). J Hazard Mater 173:502–509

Chen GQ, Zeng GM, Tang L, Du CY, Jiang XY, Huang GH, Liu HL, Shen GL (2008) Cadmium removal from simulated wastewater to biomass byproduct of *Lentinus edodes*. Bioresour Technol 99:7034–7040

Dumitru B, Laura B (2013) Sorption of Pb(II) onto a mixture of algae waste biomass and anion exchanger resin in a packed-bed column. Bioresour Technol 129:374–380

Feng J, Yang ZH, Zeng GM, Huang J, Xu HY, Zhang YY, Wei SM, Wang LK (2013) The adsorption behavior and mechanism investigation of

Pb(II) removal by flocculation using microbial flocculant GA1. Bioresour Technol 148:414–421
Fu FL, Wang Q (2011) Removal of heavy metal ions from wastewaters: a review. J Environ Manag 92:407–418
Ghorai S, Sinhamahpatra A, Sarkar A, Panda AB, Pal S (2012) Novel biodegradable nanocomposite based on XG-g-PAM/SiO2: application of an efficient adsorbent for Pb^{2+} ions from aqueous solution. Bioresour Technol 119:181–190
Guo JY, Yang CP, Peng LY (2014) Preparation and characteristics of bacterial polymer using pre-treated sludge from swine wastewater treatment plant. Bioresour Technol 152:490–498
Guo JY, Yang CP, Zeng GM (2013) Treatment of swine wastewater using chemically modified zeolite and bioflocculant from activated sludge. Bioresour Technol 143:289–297
Gupta VK, Rastogi A (2008) Biosorption of lead from aqueous solutions by green algae *Spirogyra* species: kinetics and equilibrium studies. J Hazard Mater 152:407–414
Hao YM, Man C, Hu ZB (2010) Effective removal of Cu (II) ions from aqueous solution by amino-functionalized magnetic nanoparticles. J Hazard Mater 184:392–399
Huang W, Liu ZM (2013) Biosorption of Cd(II)/Pb(II) from aqueous solution by biosurfactant-producing bacteria: isotherm kinetic characteristic and mechanism studies. Colloids Surf B Biointerfaces 105: 113–119
Huang J, Yang ZH, Zeng GM, Ruan M, Xu HY, Gao WC, Luo YL, Xie HM (2012) Influence of composite flocculant of PAC and MBFGA1 on residual aluminum species distribution. Chem Eng J 191:269–277
Jiang M, Jin X, Lu X, Chen Z (2010) Adsorption of Pb(II), Cd(II), Ni(II) and Cu(II) onto natural kaolinite clay. Desalination 252:33–39
Karatas M (2012) Removal of Pb(II) from water by natural zeolitic tuff: kinetics and thermodynamics. J Hazard Mater 199:383–389
Karthikeyan S, Balasubramanian R, Iyer CSP (2007) Evaluation of the marine algae *Ulva fasciata* and *Sargassum* sp. for the biosorption of Cu(II) from aqueous solutions. Bioresour Technol 98:452–455
Lee BJ, Schlautman MA, Toorman E, Fettweis M (2012) Competition between kaolinite flocculation and stabilization in divalent cation solutions dosed with anionic polyacrylamides. Water Res 46:5696–5706
Li Z, Zhong S, Lei HY, Chen RW, Yu Q, Li HL (2009) Production of a novel bioflocculant by *Bacillus licheniformis* X14 and its application to low temperature drinking water treatment. Bioresour Technol 100:3650–3656
Liu Y, Liu YJ (2008) Biosorption isotherms, kinetics and thermodynamics. Sep Purif Technol 61:229–242
Liu WJ, Wang K, Li BZ, Yuan HL, Yang JS (2010) Production and characterization of an intracellular bioflocculant by *Chryseobacterium daeguense* W6 cultured in low nutrition medium. Bioresour Technol 101:1044–1048
Lu XQ (2008) Thermodynamic and isotherm studies of the biosorption of Cu(II), Pb(II), and Zn(II) by leaves of saltbush (*Atriplex canescens*). J Chem Thermodyn 40:739–740
Lodeiro P, Barriada JL, Herrero R, Sastre de Vicente ME (2006) The marine macroalga *Cystoseira baccata* as biosorbent for cadmium(II) and lead(II) removal: kinetic and equilibrium studies. Environ Pollut 142:264–273
Meunier N, Drogui P, Montane C, Hausler R, Mercier G, Blais JF (2006) Comparison between electrocoagulation and chemical precipitation for metals removal from acidic soil leachate. J Hazard Mater 137: 581–590
Moon SH, Park CS, Kim YJ, Park YI (2006) Biosorption isotherms of Pb (II) and Zn(II) on Pestan, an extracellular polysaccharide, of *Pestalotiopsis* sp. KCTC 8637P. Process Biochem 41:312–316
More TT, Yan S, Hoang NV, Tyagi RD, Surampalli RY (2012) Bacterial polymer production using pre-treated sludge as raw material and its flocculation and dewatering potential. Bioresour Technol 121:425–431
Nasir MH, Nadeem R, Akhtar K, Hanif MA, Khalid AM (2007) Efficacy of modified distillation sludge of rose (*Rosa centifolia*) petals for Pb(II) and Zn(II) removal from aqueous solutions. J Hazard Mater 147:1006–1014
Pehlivan E, Altun T (2006) The study of various parameters affecting the ion exchange of Cu^{2+}, Zn^{2+}, Ni^{2+}, Cd^{2+}, and Pb^{2+} from aqueous solution on Dowex50W synthetic resin. J Hazard Mater B134:149–156
Pehlivan E, Altun T, Parlay S (2009) Utilization of barley straws as biosorbents for Cu^{2+} and Pb^{2+} ions. J Hazard Mater 164:982–986
Riahi K, Thayer BB, Mammou AB, Ammar AB (2009) Biosorption characteristics of phosphates from aqueous solution onto *Phoenix dactylifera* L. date palm fibers. J Hazard Mater 170:511–519
Sari A, Mendil D, Tuzen M, Soylak M (2008) Biosorption of Cd(II) and Cr(III) from aqueous solution by moss (*Hylocomium splendens*) biomass: equilibrium, kinetic and thermodynamic studies. Chem Eng J 144:1–9
Sari A, Tuzen M (2008) Biosorption of total chromium from aqueous solution by red algae (*Ceramium virgatum*): equilibrium, kinetic and thermodynamic studies. J Hazard Mater 160:349–355
Sari A, Tuzen M (2009) Kinetic and equilibrium studies of biosorption of Pb(II) and Cd(II) from aqueous solution by macrofungus (*Amanita rubescens*) biomass. J Hazard Mater 164:1004–1011
Sari A, Tuzen M, Uluozlu OD, Soylak M (2007) Biosorption of Pb(II) and Ni(II) from aqueous solution by lichen (*Cladonia furcata*) biomass. Biochem Eng J 37:151–158
Senthilkumar R, Vijayaraghavan K, Thilakavathi M, Iyer PVR, Velan M (2007) Application of seaweeds for the removal of lead from aqueous solution. Biochem Eng J 33:211–216
Sun J, Zhang XH, Miao XJ, Zhou JT (2012) Preparation and characteristics of bioflocculants from excess biological sludge. Bioresour Technol 126:362–366
Tunali S, Akar T, Ozcan SA, Kiran I, Ozcan A (2006) Equilibrium and kinetics of biosorption of lead(II) from aqueous solutions by *Cephalosporium aphidicola*. Sep Purif Technol 47:105–112
Uluozlu OD, Sari A, Tuzen M, Soylak M (2008) Biosorption of Pb(II) and Cr(III) from aqueous solution by lichen (*Parmelina tiliaceae*) biomass. Bioresour Technol 99:2972–2980
Velmurugan N, Hwang G, Sathishkumar M, Choi TK, Lee KJ, Oh BT, Lee YS (2010) Isolation, identification, Pb(II) biosorption isotherms and kinetics of a lead adsorbing *Penicillium* sp. MRF-1 from South Korean mine soil. J Environ Sci 22:1049–1056
Wan MW, Kan CC, Robel BD, Dalida MLP (2010) Adsorption of copper (II) and lead (II) ions from aqueous solution on chitosan-coated sand. Carbohydr Polym 3:891–899
Widiastuti N, Wu HW, Ang HM, Zhang DK (2011) Removal of ammonium from greywater using natural zeolite. Desalination 277:15–23
Witek-Krowiak A, Szafran RG, Modelski S (2011) Biosorption of heavy metals from aqueous solutions onto peanut shell as a low-cost biosorbent. Desalination 265:126–134
Yahya SK, Zakaria ZA, Samin J, Raj ASS, Ahmad WA (2012) Isotherm kinetics of Cr(III) removal by non-viable cells of *Acinetobacter haemolyticus*. Colloids Surf B: Biointerfaces 94:362–368
You Y, Ren N, Wang A, Ma F, Gao L, Peng Y, Lee D (2008) Use waste fermenting liquor to produce bioflocculants with isolated strains. Int J Hydrogen Energy 33:3295–3301
Yuvaraja G, Krishnaiah N, Subbaiah MV, Krishnaiah A (2014) Biosorption of Pb(II) from aqueous solution by *Solanum melongena* leaf powder as a low-cost biosorbent prepared from agricultural waste. Colloids Surf B: Biointerfaces 114:75–81